

See discussions, stats, and author profiles for this publication at: <https://www.researchgate.net/publication/5306311>

# Proteomic Analysis Identifies Protein Targets Responsible for Depsipeptide Sensitivity in Tumor Cells

ARTICLE *in* JOURNAL OF PROTEOME RESEARCH · AUGUST 2008

Impact Factor: 4.25 · DOI: 10.1021/pr7008753 · Source: PubMed

---

CITATIONS

20

READS

13

## 9 AUTHORS, INCLUDING:



[Ying Gao](#)

Population Council

6 PUBLICATIONS 28 CITATIONS

[SEE PROFILE](#)

## Proteomic Analysis Identifies Protein Targets Responsible for Depsipeptide Sensitivity in Tumor Cells

Guozhu Chen,<sup>†</sup> Ailing Li,<sup>§</sup> Ming Zhao,<sup>†</sup> Ying Gao,<sup>†</sup> Tao Zhou,<sup>§</sup> Yuanji Xu,<sup>†</sup> Zhiyan Du,<sup>†</sup> Xuemin Zhang,<sup>\*,§</sup> and Xiaodan Yu<sup>\*,†</sup>

Department of Pathology, Beijing Institute of Basic Medical Sciences, 27 Taiping Road, Beijing 100850, China,  
and National Center of Biomedical Analysis, 27 Taiping Road, Beijing, 100850, China

Received December 21, 2007

Depsipeptide FR901228 (FK228) is a new kind of histone deacetylase inhibitors (HDACi) that induces growth arrest and cell death in a variety of tumor cells. Though its effects on oncogene expression and degradation have been documented, the detailed mechanism of FK228-induced cytotoxicity is still undefined. In this study, a differential proteomic analysis was performed to identify proteins associated with FK228-induced cytotoxicity in human lung cancer cells. Two-dimensional gel electrophoresis (2-DE) revealed a distinct protein profile of H322 cells in response to FK228 treatment, and 45 protein spots with significant alteration were screened. In total, 27 proteins were identified by mass spectrometry and involved in signal transduction, transcriptional regulation, metabolism, cytoskeletal organization, and protein folding, synthesis and degradation, consistent with multiple effects of FK228 on tumor cells. Notably, a novel target protein, thioredoxin reductase (TrxR), was identified, which is downregulated in FK228-sensitive cancer cells, but upregulated in resistant cells. The expression level of TrxR was negatively correlated with ROS accumulation, DNA damage and apoptosis, implicating TrxR in FK228-induced apoptosis and HDACi sensitivity in cancer cells. Thus, proteomic analysis provides new information about target proteins important for FK228-induced cytotoxicity in cancer cells.

**Keywords:** Histone deacetylase inhibitors • depsipeptide • thioredoxin reductase • thioredoxin • heat shock protein 27 • reactive oxygen species • proteomic • apoptosis

### Introduction

Histone deacetylase inhibitors (HDACi) are promising chemotherapeutic agents, which demonstrate significant anticancer activity, including inhibition of proliferation, stimulation of differentiation and induction of apoptosis.<sup>1–3</sup> Several HDACi, including Depsipeptide (FK228), suberoylanilide hydroxamic acid (SAHA), MS-275, trichostatin A (TSA), valproic acid (VA), and LAQ824 are currently demonstrating promising results in phase I/II clinical trials both for hematological malignancies and solid tumors.<sup>4,5</sup> By facilitating gene expression, HDACi-induced histone acetylation may provide a mechanism for cancer cell cytotoxicity and explain changes to target gene expression observed from microarray analysis.<sup>6,7</sup> HDACi also induce acetylation of nonhistone proteins that regulate the stability and activity of other proteins.<sup>8</sup> HDACi-induced acetylation of HSP90, for example, promotes the degradation of multiple oncoproteins, resulting in growth arrest and death of various cancer cells.<sup>9</sup>

Compared with traditional chemotherapeutic agents, HDACi selectively target transformed or tumorigenic cells without affecting normal cells.<sup>10</sup> The IC<sub>50</sub> of FK228 against human tumor cells lies within the range several ng/mL but exceeds 1000 ng/mL for normal human fibroblasts.<sup>11</sup> Recently, some studies have shown that HDACi are also selective against different types of cancer cells.<sup>12</sup> Cancer cells with elevated E2F1 activity are highly susceptible to TSA and SAHA-induced cell death.<sup>13</sup> Leukemia cells are highly sensitive to VA treatment, which causes an upregulation of Fas, FasL, and TRAIL, inducing death receptor-mediated apoptosis in cancer cells, but not in normal hematopoietic progenitors.<sup>14</sup> HDACi also cause the selective accumulation of reactive oxygen species (ROS) in tumor cells, initiating mitochondrial-mediated apoptosis.<sup>10</sup> Though many proteins and molecules can mediate the selective cytotoxicity of HDACi in tumor cells, the underlying mechanism behind this activity remains largely undefined.

In this study, the mechanism of FK228-induced cytotoxicity was investigated by identifying the protein profile of H322 cells in response to FK228 treatment. Twenty-seven proteins with significant changes between normal and FK228-treated H322 cells were identified, which were involved in multiple biological processes including signal transduction, transcriptional regulation, metabolism, cytoskeletal organization, and protein synthesis, folding, and degradation. Thioredoxin reductase (TrxR), a novel target identified by proteomic analysis, is involved in

\* To whom correspondence should be addressed. Xiaodan Yu, Ph.D., Professor, Department of Pathology, Beijing Institute of Basic Medical Sciences, 27 Taiping Road, Beijing 100850, China. Tel, 8610-66932372; fax, 8610-68213039; e-mail, yuxd@nic.bmi.ac.cn. Xuemin Zhang, Ph.D., Professor, National Center of Biomedical Analysis, 27 Taiping Road, Beijing, 100850, China. Tel, 8610-86538178; fax, 8610-68246161; e-mail, xmzhang@nic.bmi.ac.cn.

<sup>†</sup> Beijing Institute of Basic Medical Sciences.

<sup>§</sup> National Center of Biomedical Analysis.

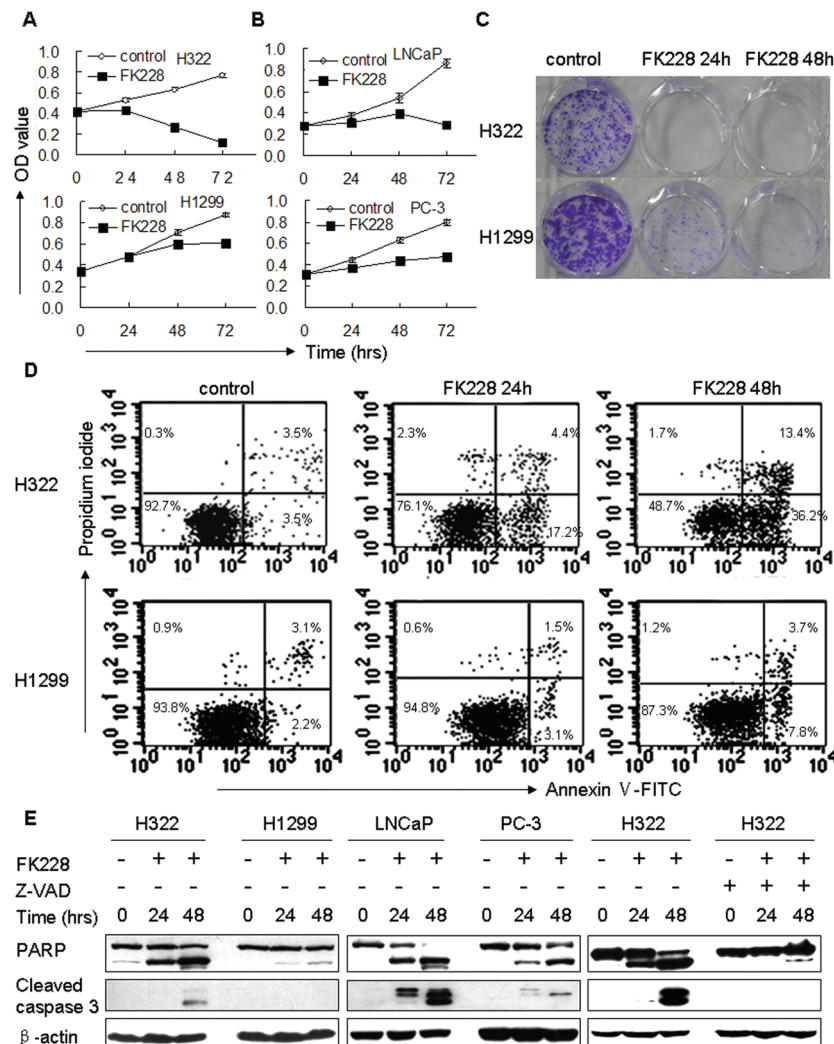


**Figure 1.** Effect of FK228 on cell growth and viability in human lung and prostate cancer cells. Lung and prostate cancer cells were treated with or without 25 ng/mL FK228 for 24 and 48 h. Cell growth inhibition was determined by MTT assay. (A) Cell growth of H322 and H1299 cells. (B) Cell growth of LNCaP and PC-3 cells. (C) Clonogenic survival assay. One thousand H322 or H1299 cells were plated per well in 6-well plates for 72 h, followed by FK228 treatment for the indicated times. Cells were washed, given fresh media, and stained with crystal violet after 12 days. Representative plates are shown. (D) Apoptosis of lung cancer cells. H322 and H1299 cells were treated with or without 25 ng/mL FK228 and harvested at the indicated time point. The collected cells were stained with annexin V-FITC and propidium iodide and analyzed by flow cytometry. (E) Caspase-dependent apoptosis of lung and prostate cancer cells. Cells were cultured with (+) or without (-) 25 ng/mL FK228 in the presence (+) or absence (-) of 50 μM Z-VAD-FMK for the indicated times. PARP and cleaved caspase 3 were analyzed by Western blotting; β-actin was used as loading control.

regulating apoptosis and determining HDACi sensitivity in tumor cells. These results illustrate the utility of differential proteomic analysis for obtaining new information and illuminating the mechanism of HDACi-induced cancer cell cytotoxicity.

## Results

**FK228 Induces Time-Dependent Growth Arrest and Apoptosis in Lung and Prostate Cancer Cells.** As a new kind of HDACi, FK228 has shown strong anticancer activity in clinical trials.<sup>15,16</sup> In this study, we evaluate the effect of FK228 on the growth and apoptosis of nonsmall cell lung cancer (NSCLC) and prostate cancer cells. NSCLC (H322 and H1299) and prostate cancer (LNCaP and PC-3) cells were treated with 25 ng/mL FK228 for the indicated times, and MTT assay was used to evaluate cell growth inhibition. The results indicate that FK228 completely inhibits proliferation of H322 and LNCaP

cells, but only partially blocks proliferation of H1299 and PC-3 cells (Figure 1A,B). The impact of FK228 on cell survival was further determined by clonogenic survival assays. As Figure 1C shows, FK228 significantly inhibits colony formation in lung cancer cells, especially in H322 cells. FK228-induced apoptotic cell death was confirmed by annexin V-FITC staining; after 48 h of FK228 treatment, apoptotic rates of H322 and H1299 rose to 49.65% and 10.48%, respectively (Figure 1D). Cleaved PARP and caspase-3 were analyzed by Western blotting to determine whether FK228-induced apoptosis is caspase-dependent (Figure 1E). The results indicate that FK228 markedly increases PARP and caspase-3 cleavage in H322 and LNCaP cells, but this effect was less significant in PC-3 and H1299 cells. With the presence of Z-VAD-FMK, a pan-caspase inhibitor, the effect of FK228 on PARP and caspase-3 cleavage was completely inhibited, indicating that FK228 induces apoptosis by activating the caspase pathway.

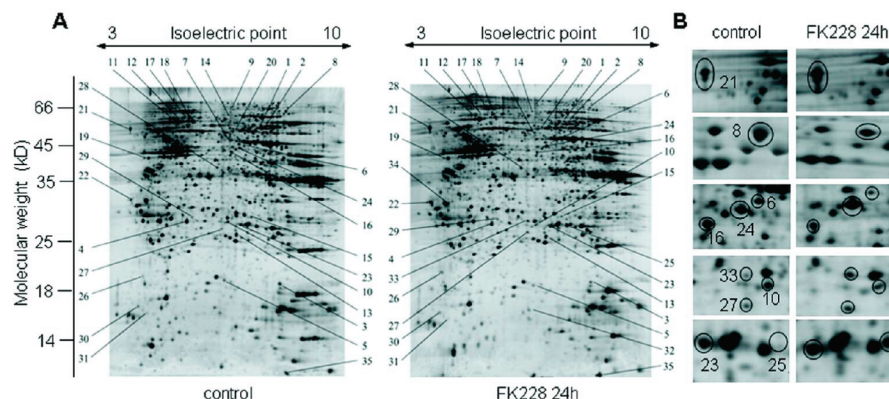


**Figure 2.** 2-DE analyses of differentially expressed protein spots between control and FK228-treated H322 cells. (A) 2-DE analysis of differentially expressed protein spots. Total cell lysates ( $130\ \mu\text{g}$ ) extracted from control and FK228-treated H322 cells were subjected to 2-DE analysis and detected by silver staining. The approximate isoelectric points (pI) and molecular masses (kDa) of the proteins are indicated at the top and left, respectively. The marked protein spots represent the identified proteins listed in Table 1. (B) Close-up sections of some identified protein spots. The compared sections are magnified images of silver-stained 2-D gels, and the number of protein spot is the same as shown in Table 1.

Collectively, FK228 induces time-dependent growth arrest and apoptosis in lung and prostate cancer cells. Moreover, H322 and LNCaP cells are sensitive to FK228 treatment while H1299 and PC-3 cells are relatively resistant.

**Proteomic Assay to Identify the Differentially Expressed Proteins Induced by FK228.** The protein profile of H322 cells in respond to FK228 treatment was determined by 2-DE and MALDI-TOF-MS. More than 1200 protein spots were detected on the silver stain gel, and 45 protein spots with significant alteration were selected for identification (Figure 2A). Of these, 35 protein spots representing 27 unique proteins were identified with significant Peptides Mass Fingerprinting (PMF) values ( $p < 0.05$ ). The identified protein spots include 20 downregulated and 15 upregulated protein spots (Table 1). Close-up sections for several identified proteins reveal a significant alteration in spot appearance after FK228 treatment (Figure 2B).

**Cluster of Identified Proteins.** The identified proteins were classified into five clusters according to their biological function. The clusters include signal transduction, transcriptional regulation, metabolism, cytoskeletal protein, and protein folding, synthesis and degradation (Table 2). The transcriptional regulation cluster contains six proteins which all decreased after FK228 treatment. HSP27 and calreticulin (CRT), two chaperone proteins that promote protein folding and regulate apoptosis, were, respectively, down- and upregulated in response to FK228. Most proteins in the metabolism cluster are associated with energy biosynthesis, especially pyruvate kinase isozyme M1/M2 (PKM2), which is the key enzyme regulating energy production in tumor cells.<sup>17</sup> Most proteins that regulate energy production were depleted by FK228. TrxR, which plays a key role in scavenging ROS, decreased in H322 cells treated with FK228. The cluster of cytoskeletal proteins consists of six proteins, most of which were cleaved into two or three protein fragments in cells treated with FK228.

**Confirmation of Some Identified Proteins by RT-PCR and Western Blotting.** Proteins related to tumorigenesis or apoptosis were selected from the list of identified proteins for further study. There were 10 proteins that matched these criteria: TrxR, HSP27, CRT, PKM2, heterogeneous nuclear ribonucleoprotein K (hnRNP K), far upstream element-binding protein 1 (FBP), high-mobility group box 1 variant (HMGB1), ras-GTPase-activating protein SH3-domain-binding protein

(G3BP), reticulocalbin 1 (RCN1), and growth factor receptor-bound protein 2 isoform 1 (GRB2). The alterations of these proteins determined by proteomic analysis were verified using RT-PCR and Western blotting (Figure 3). Nine of the 10 proteins tested with RT-PCR and five of the six proteins detected by Western blotting confirmed the proteomic analysis accurately reflects the alteration of proteins at the transcriptional and protein levels in response to FK228. CRT and HMGB1 were the exceptions, both with an inhibition at the transcriptional level, but an enhancement of CRT and no changes of HMGB1 at the protein level. We assumed that FK228-induced acetylation modifications may account for the discrepancy as acetylation could alter the electric charge and stability of proteins.

**Effect of FK228 and SAHA on the Expression of TrxR, HSP27, CRT and GRB2 in Lung and Prostate Cancer Cell Lines.** To determine whether the alteration of TrxR, HSP27, CRT, and GRB2 were associated with HDACi sensitivity in cancer cells, we evaluated the alteration of the four proteins in HDACi-sensitive (H322 and LNCaP) and resistant (H1299 and PC-3) cancer cells treated with FK228 or SAHA. The results indicated that FK228 and SAHA had a similar effect on the alteration of the four proteins. CRT and GRB2 were upregulated by both FK228 and SAHA in all four cell lines. FK228 and SAHA attenuated TrxR in HDACi-sensitive cancer cells, but increased TrxR in HDACi-resistant cancer cells. HSP27 decreased in HDACi-sensitive cancer cells, but underwent no significant changes in HDACi-resistant cancer cells after FK228 and SAHA treatment (Figure 4). On the basis of these results, we assume that TrxR and HSP27 may be involved in determining the sensitivity of cancer cells to the cytotoxicity of HDACi.

**Effect of HSP27 on FK228-Induced Apoptosis.** HSP27 is a chaperone protein that facilitates protein folding and inhibits caspase-dependent apoptosis.<sup>18</sup> FK228 shows differential regulation of HSP27 expression between sensitive and resistant cells, which suggests that HSP27 may be a key target mediating FK228-induced cytotoxicity. First, the HSP27 expression plasmid was transfected into H322 cells. As Figure 5A shows, the overexpression of HSP27 did not inhibit FK228-induced PARP cleavage. Next, siRNA transfection was used to deplete HSP27 in H1299 cells. Compared with nonsilencing siRNA, HSP27 siRNA significantly decreased the level of HSP27 in H1299 cells. However, the depletion of HSP27 did not enhance FK228-

**Table 1.** List of Proteins Identified by Mass Spectrometry Significantly Changed between Control and FK228-Treated Cells<sup>a</sup>

spot no.	protein name	NCBI ID no.	abbr. name	$M_r$ (kDa)		pI	obsrv.	theor.	sequence coverage (%)	score	protein expression
				obsrv.	theor.						
1	Aldehyde dehydrogenase 1 family, member A3	AAH63274	ALDH1A3	56.073	58.987	6.99	6.42	24%	101	→	↑
2	Aldehyde dehydrogenase 1 family, member A3	AAH63274	ALDH1A3	56.073	58.900	6.99	6.52	23%	116	→	↑
3	Basic transcription factor 3 isoform B	NP_001198	BTF3	17.688	19.854	6.85	7.58	67%	96	→	↑
4	Beta actin variant	BAD96752	$\beta$ -actin	41.738	27.953	5.37	5.58	37%	80	→	↑
5	BTF3L4 protein	AAH21004	BTF3L4	16.461	19.457	5.41	6.01	51%	77	→	↑
6	Chain C, Ornithine Aminotransferase Mutant Y85i	2BYJ_C	Orn-AT-Y85I	48.454	46.214	6.57	6.18	31%	81	→	↑
7	Dnaj subfamily A member 2	NP_005871	DNAJ2	45.717	49.982	6.06	6.08	39%	128	→	↑
8	Far upstream element-binding protein 1	Q96AE4	FBP	67.431	70.970	7.18	7.44	37%	106	→	↑
9	Glycyl-tRNA synthetase	AAA68443	GlyRS	77.463	78.153	5.88	6.15	33%	133	→	↑
10	Heat shock protein 27	AAA62175	HSP 27	22.313	27.699	7.83	6.12	52%	97	→	↑
11	Heterogeneous nuclear ribonucleoprotein K	CAI16022	hnRNP K	41.781	62.953	5.43	5.28	21%	68	→	↑
12	Heterogeneous nuclear ribonucleoprotein K	CAI16019	hnRNP K	47.528	63.609	5.46	5.48	42%	111	→	↑
13	High-mobility group box 1 variant	BAD92235	HMGB1	20.151	25.909	9.75	6.22	44%	68	→	↑
14	Leukotriene A4 hydrolase	NP_000886	LTA4H	69.241	65.907	5.8	5.92	42%	180	→	↑
15	Phosphoglycerate mutase 1	NP_002620	PGAM1	28.786	29.079	6.67	6.37	66%	129	→	↑
16	Pyruvate kinase isozymes M1/M2	P14618	PKM2	57.769	44.077	7.95	6.16	30%	85	→	↑
17	Ras-GTPase-activating protein SH3-domain-binding protein	NP_005745	G3BP	52.132	65.228	5.36	5.52	36%	67	→	↑
18	Ras-GTPase-activating protein SH3-domain-binding protein	NP_005745	G3BP	52.132	65.421	5.36	5.59	36%	76	→	↑
19	reticulocalbin 1 precursor	NP_002892	RCN1	38.866	41.455	4.86	4.78	36%	74	→	↑
20	Thioredoxin reductase 1, cytoplasmic precursor	Q16881	TR	54.672	55.434	6.07	6.17	58%	197	→	↑
21	Calreticulin precursor variant	BAD96780	CRT	46.890	55.189	4.30	4.34	48%	94	→	↑
22	Calreticulin precursor variant	BAD96780	CRT	46.890	31.565	4.30	4.41	48%	94	→	↑
23	Chain B, Triosephosphate Isomerase	IHTL_B	TP1	26.522	27.511	6.51	6.26	37%	102	→	↑
24	Chain C, Ornithine Aminotransferase Mutant Y85i	2BYJ_C	Orn-AT-Y85I	48.454	44.729	6.57	6.21	34%	134	→	↑
25	Cytokeratin 18	CAA31377	CK-18	47.305	27.805	5.27	6.61	33%	98	→	↑
26	Cytokeratin 18	CAA31377	CK-18	47.305	21.027	5.27	4.64	26%	76	→	↑
27	Growth factor receptor-bound protein 2 isoform 1	NP_002077	GRB2	25.190	26.566	5.89	5.81	39%	65	→	↑
28	Isocitrate dehydrogenase 3 (NAD+) alpha	AAH21967	IDH3A	39.566	38.822	6.47	5.78	24%	78	→	↑
29	Cytokeratin 19	P08727	CK-19	44.065	28.641	5.04	5.62	36%	107	→	↑
30	Cytokeratin 19	P08727	CK-19	44.065	16.818	5.04	4.59	50%	175	→	↑
31	Cytokeratin 19	P08727	CK-19	44.065	16.311	5.04	4.82	23%	144	→	↑
32	Cytokeratin 1	KRHU2	CK-1	65.454	17.049	6.03	5.87	31%	91	→	↑
33	Lamin A/C	CAI15520	Lamin A/C	53.219	28.338	6.13	5.84	27%	73	→	↑
34	Tropomyosin 3 isoform 2	XP_865669	TPM3	27.158	31.302	4.77	4.82	35%	115	→	↑
35	Ubiquitin	751846A	Ubq	8.446	12.196	6.56	6.04	63%	70	→	↑

<sup>a</sup>The calculation of observed pI and  $M_r$  was based on the migration of the protein spot on 2-D gels. The arrows (↑ and ↓) mean the protein increased and decreased in FK228 treated cells, respectively. The spot numbers correspond to those on the 2-DE images shown in Figure 2.

**Table 2.** Functional Classification of the Identified Proteins Significantly Changed between Control and FK228-Treated Cells

functional group	protein ID	function
Signal transduction	GRB2	Adapter protein that provides a critical link between cell surface growth factor receptors and the Ras signaling pathway
Transcription	FBP	Regulates MYC expression by binding to a single-stranded far-upstream element (FUSE) upstream of the MYC promoter
Transcription	hnRNP K	Likely to play a role in the nuclear metabolism of hnRNAs, particularly for pre-mRNAs that contain cytidine-rich sequences
Transcription	G3BP	Cleaves c-myc mRNA preferentially at the 3'UTR, includes ATP and magnesium-dependent helicase
Transcription	HMGB1	Binds preferentially single-stranded DNA, unwinds double-stranded DNA and regulates the transcriptional preinitiation complex formation
Transcription	BTTF3L4	Can form a stable complex with RNA polymerase II, required for the initiation of transcription
Transcription	BTTF3	Form a stable complex with RNA polymerase II. Required for the initiation of transcription
Protein biosynthesis	GlyRS	Catalyze conversion of glycyl-tRNA and regulatin protein biosynthesis
Protein biosynthesis	LTA4H	Hydrolyzes an epoxide moiety of leukotriene A4 (LTA-4) to form leukotriene B4 (LTB-4)
Protein folding	CRT	Molecular calcium binding chaperone promoting folding, oligomeric assembly in the ER via the calreticulin/calnexin cycle
Protein folding	RCN1	May regulate calcium-dependent activities in the endoplasmic reticulum lumen or post-ER compartment
Protein folding	HSP 27	Involved in stress resistance and actin organization
Protein folding	DNAJA2	Cochaperone of Hsc70 and involved in the regulation of protein folding and cell proliferation
Protein degradation	Ubq	It is involved in ATP-dependent nonlysosomal proteolysis and regulation of chromatin structure and transcriptional activity
Metabolism	ALDH1A3	Recognizes substrates free retinal and cellular retinol-binding protein-bound retinal
Metabolism	Orn-AT-Y85I	Regulates amino acid and ornithine metabolism
Metabolism	PGAM1	Interconversion of 3- and 2-phosphoglycerate with 2,3-bisphosphoglycerate
Metabolism	PKM2	It is a key enzyme in the energetical metabolism which catalyzes the conversion of pyruvate to phosphoenolpyruvate
Metabolism	TPI1	Catalyzes the aldose-ketose isomerization of dihydroxyacetone phosphate and glyceraldehyde 3-phosphate
Metabolism	IDH3A	Catalyzes the conversion of isocitrate and 2-oxoglutarate, regulate TCA circulation
Metabolism	TR	Catalyzes the reduction of Thioredoxin as well as numerous other oxidized cellular proteins which play an important role in the redox regulation of multiple intracellular processes
Cytoskeletal protein	$\beta$ -actin	Involved in various types of cell motility and ubiquitously expressed in all eukaryotic cells
Cytoskeletal protein	CK-18	Forming intermediate fiber and regulating cell mobility
Cytoskeletal protein	CK-19	Forming cytoskeleton and regulating cell communication
Cytoskeletal protein	CK-1	Regulating cell communication and responding to oxidative stress
Cytoskeletal protein	Lamin A/C	Provide a framework for the nuclear envelope and may also interact with chromatin
Cytoskeletal protein	TPM3	Binds to actin filaments and plays a central role in the regulation of vertebrate striated muscle contraction and stabilizing cytoskeleton actin filaments

induced PARP cleavage (Figure 5B). These results indicate that the changes in HSP27 were not involved in FK228-induced apoptosis.

**Effect of FK228 on the Protein Level and Activity of TrxR, ROS Accumulation, and DNA Damage in Lung Cancer Cells.** Trx is the substrate of TrxR and has been reported to determine HDACi sensitivity in normal and cancer cells.<sup>10</sup> Therefore, we wanted to test whether a similar mechanism was responsible for the differential HDACi sensitivities in our current study. The alteration of TrxR and Trx was determined after prolonged treatment with FK228 for 48 h.

The results indicate that FK228 decreases TrxR in H322 cells in a time-dependent manner, but increases TrxR in H1299 cells after 24 h in culture. In contrast, the alteration of Trx decreases in H1299 cells and slightly increases in H322 cells after FK228 treatment (Figure 6A). As a reductase, the function of TrxR depends entirely on its reducing activity.<sup>19</sup> Because FK228 differentially regulates the protein levels of TrxR in HDACi-sensitive and resistant cancer cells, we decided to look at how TrxR activity changes between H322 and H1299 cells. The results show that TrxR activity significantly decreases in H322 cells at 48 h, but markedly increases

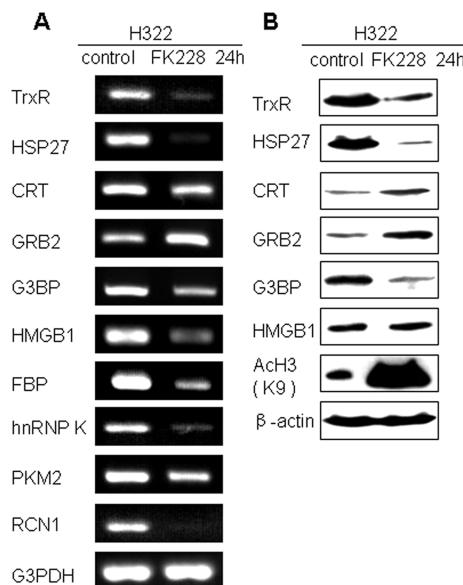


**Figure 3.** Confirmation of several differentially expressed proteins at the transcriptional and translational levels. H322 cells were treated with or without 25 ng/mL FK228. After 24 h, cells were collected for analysis by RT-PCR and Western blotting. (A) mRNA levels of 10 identified proteins. Total RNA was prepared from control and FK228-treated cells. RT-PCR was performed with specific primers for TrxR, HSP27, CRT, GRB2, hnRNP K, G3BP, FBP, HMGB1, PKM2, and RCN1; G3PDH was used as loading control. (B) Protein levels of six identified proteins. The total proteins were extracted from control and FK228-treated H322 cells. Western blotting was performed with the specific antibody of TrxR, HSP27, CRT, GRB2, G3BP and HMGB1;  $\beta$ -actin was used as loading control.

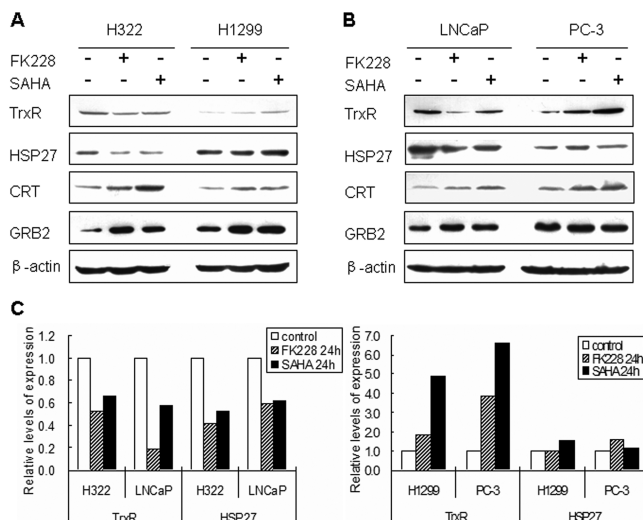


**Figure 4.** Effect of FK228 and SAHA on the expression of TrxR, HSP27, CRT and GRB2 in lung and prostate cancer cells. H322, H1299, LNCaP and PC-3 cells were cultured with (+) or without (-) 25 ng/mL FK228 or 2  $\mu$ M SAHA for 24 h. Western blotting was used to analyze the expression of TrxR, HSP27, CRT and GRB2 in lung (A) and prostate (B) cancer cells;  $\beta$ -actin was used as loading control. The relative levels of each protein were shown as ratio compare with control group (C).

in H1299 cells after 24 h of FK228 treatment (Figure 6B). The alteration of TrxR activity matches the changes in TrxR protein level.

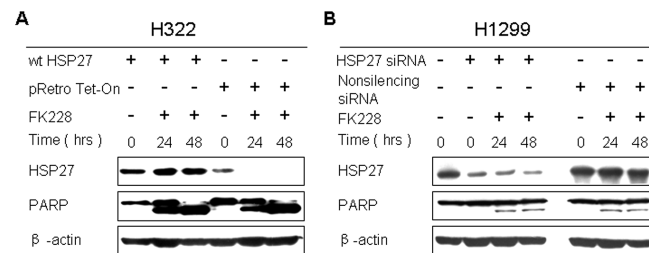


**Figure 5.** Effect of HSP27 on the caspase-dependent apoptosis induced by FK228 in lung cancer cells. (A) Effect of HSP27 overexpression on the cleavage of PARP. H322 cells were transfected with wild type human HSP27 vectors (wtHSP27) or empty vectors (pRetro Tet-On) for 24 h and then treated with (+) or without (-) 25 ng/mL FK228 for the indicated times. Western blot analysis of HSP27 and PARP is shown;  $\beta$ -actin was used as loading control. (B) Effect of HSP27 depletion on the cleavage of PARP. H1299 cells were transfected with 100 nM HSP27 siRNA or nonsilencing siRNA for 24 h and then treated with (+) or without (-) 25 ng/mL FK228 for the indicated times. Protein levels of HSP27 and PARP were analyzed by Western blotting;  $\beta$ -actin was used as loading control.

Because TrxR and Trx play key roles in scavenging ROS, we next measured the alteration of ROS in H322 and H1299 cells following FK228 treatment. Fluorescence microscopy and flow cytometry results both demonstrate that FK228 induces ROS accumulation in a time-dependent manner for both H322 and H1299 cells, but the changes in H322 cells were more significant (Figures 6C,D). Obviously, the depletion of TrxR contributes to ROS accumulation in H322 cells, while the depletion of Trx causes ROS accumulation in H1299. On the other hand, the persistence of TrxR in H1299 cells may compensate for effects on Trx, which would explain why ROS accumulation in H1299 cells was less significant than in H322 cells. Aberrant ROS can induce DNA damage,<sup>20</sup> which activates the expression of phospho-H2AX.<sup>21</sup> We therefore looked for changes to phospho-H2AX in H322 and H1299 cells. FK228 induces time-dependent increase in the number of cells testing positive for phospho-H2AX in both H322 and H1299 cells. As Figure 6E shows, FK228 induces DNA damage in lung cancer cells, but DNA damage in H322 cells was more significant than in H1299 cells, similar to the patterns observed for ROS accumulation in these cells.

The above results suggest a molecular mechanism for the differential sensitivity of cancer cells to FK228 treatment. In sensitive cells, FK228 mainly targets TrxR, decreasing its activity and causing ROS accumulation and DNA damage. In resistant cells, however, FK228 primarily downregulates Trx, which may play a less significant role in scavenging ROS than TrxR.

**Effect of TrxR on FK228-Induced ROS Accumulation and Apoptosis.** To further confirm this hypothesis, we used siRNA to knock down TrxR in H1299 and measured the effect on resistance to FK228 treatment. As shown in Figure 7A, TrxR siRNA significantly depleted TrxR in H1299 cells compared to nonsilencing siRNA and resulted in a significant enhancement of FK228-induced PARP cleavage. Reduction of TrxR also increased ROS accumulation in response to FK228 treatment as determined by fluorescence microscopy and flow cytometry (Figure 7B,C). These results demonstrate that the depletion of TrxR enhances the sensitivity of H1299 cells to FK228-induced ROS accumulation and apoptosis, supporting the hypothesis that TrxR is a key target protein that determines HDACi sensitivity in cancer cells by regulating cellular redox.

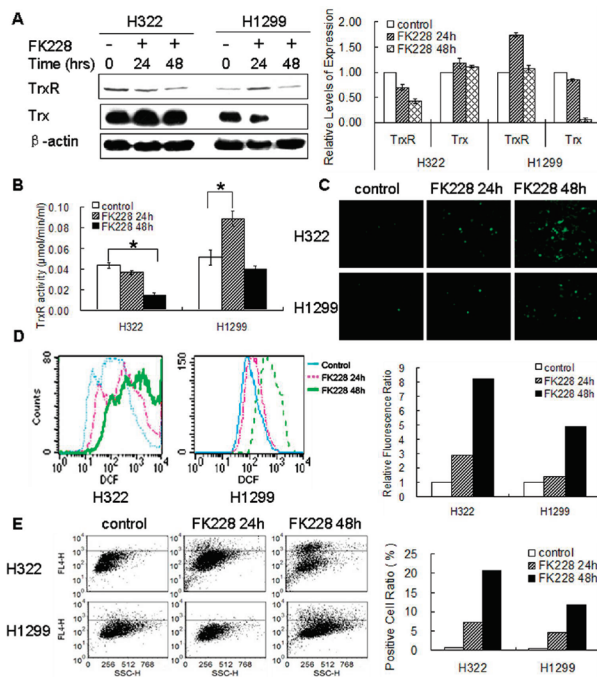


**Figure 6.** Effect of FK228 on antioxidant defense system, ROS accumulation and DNA damage in lung cancer cells. (A) Expression of TrxR and Trx. H322 and H1299 cells were cultured with (+) or without (-) 25 ng/mL FK228 for 24 and 48 h. Western blot analysis of TrxR and Trx are shown;  $\beta$ -actin was used as loading control. The relative levels of each protein are shown as a ratio against the control group and represent the average values of three independent experiments. (B) TrxR activity in H322 and H1299 cells. H322 and H1299 cells were cultured with or without 25 ng/mL FK228 for the indicated times. TrxR activity was measured by thioredoxin reductase 1 assay kit according to the manufacturer's instruction and displayed as a histogram. All columns display mean  $\pm$  SD of data from three independent experiments. \* $P$  < 0.05 compared with control cells. (C) ROS accumulation observed by fluorescence microscope. H322 and H1299 cells were treated with or without 25 ng/mL FK228 for the indicated times and stained with DCFH-DA for 1 h. ROS were labeled with DCF and observed by fluorescence microscope. (D) ROS accumulation measured by flow cytometry. H322 and H1299 cells were treated with or without 25 ng/mL FK228 for the indicated times and stained with DCFH-DA for 1 h. Cells were labeled with DCF and analyzed by flow cytometry. (E) Expression of phospho-H2A.X (ser 139). Lung cancer cells were treated with or without 25 ng/mL FK228 for the indicated times and collected by trypsinization. After fixation, permeabilization and blockage, cells were labeled with antibody of Phospho-Histone H2A.X (Ser139) and analyzed by flow cytometry. The positive cell ratio is shown as a histogram.

## Discussion

FK228 is one of a new generation of chemotherapeutic agents that has demonstrated encouraging results in phase I/II clinical trials,<sup>15,16</sup> but the mechanism of FK228-induced cytotoxicity remains largely undefined. Using proteomic analysis, we investigated the mechanism of FK228 action and identified 27 proteins whose expression changes significantly in response to FK228 treatment. These proteins are associated with multiple biological functions, suggesting that diverse mechanisms regulate FK228-induced cytotoxicity. Similarly, microarray analysis of tumor cells has identified hundreds of genes that are differentially regulated in response to FK228 and associated with multiple signaling pathways.<sup>6,7</sup>

Some of the proteins identified in the signal transduction, protein folding, and cytoskeletal protein clusters were regulated in a manner that facilitates FK228-induced growth arrest and apoptosis. GRB2 is an adaptor protein that plays a key role in activating the MAPK signaling pathway, but overexpression of GRB2 inhibits cell proliferation by suppressing the phosphorylation of PLC- $\gamma$ 1 and promoting the degradation of mutant EGFR.<sup>22,23</sup> Therefore, the upregulation of GRB2 in lung and prostate cancer cells after treatment with FK228 may partially explain the reduction of proliferation. CRT, a multifunctional,  $\text{Ca}^{2+}$ -binding chaperone in the endoplasmic reticulum, facilitates apoptosis by activating calcineurin through its regulation of  $\text{Ca}^{2+}$  release.<sup>24</sup> Overexpression of CRT enhances the sensitivity of glioblastoma cells to irradiation-induced apoptosis,<sup>25</sup> and CRT is reported to suppress tumor growth by inhibiting angiogenesis.<sup>26</sup> In this study, CRT was upregulated by both FK228 and SAHA in lung and prostate cancer cells, demonstrating that it is a common HDACi-regulated protein; however, further investigation is necessary to determine whether enhanced expression of CRT leads to an inhibition of angiogenesis in response to HDACi. Cytoskeletal proteins play a key role in maintaining cell morphology. Some of the cytoskeletal proteins, including cytokeratin-18 (CK-18) and cytokeratin-19 (CK-19), are substrates of caspase-3 and are, therefore, cleaved in tumor cells treated with cytotoxic agents.<sup>27,28</sup> In this study, most of the cytoskeletal proteins that were identified, including CK-18 and CK-19, were cleaved into two or three protein spots after treatment with FK228, which explains the morphological changes associated with caspase-dependent apoptosis induced by FK228.

Energy deficiency and inhibition of oncogene expression were involved in FK228-induced cell proliferation inhibition and death. Cell division is a biological process that requires large amounts of energy, so limiting energy synthesis can often result in growth arrest or cell death.<sup>17</sup> FK228 causes a dramatic reduction in proteins necessary for energy production, suggesting that energy deficiency may provide another important mechanism for FK228-mediated cell death. Finally, hnRNP K, G3BP, and FBP bind DNA or RNA to initiate the expression of many genes, most notably the oncogene *myc*, which promotes cell growth and transformation.<sup>29–32</sup> Moreover, G3BP is a downstream effector of Ras signaling, which is highly overexpressed in breast cancer cells and promotes cell cycle progression.<sup>33</sup> The downregulation of these three proteins may also facilitate the growth arrest of tumor cells in response to FK228.

HSP27 is differentially expressed in HDACi-sensitive and resistant tumor cells, but the alteration of HSP27 had no effect on FK228-induced apoptosis. HSP27 is a chaperone protein that inhibits mitochondrial-mediated apoptosis by binding cytochrome c and suppressing the formation of the apoptosome complex.<sup>18</sup> It has been reported that overexpression of HSP27 blocks glucocorticoid-evoked apoptosis in hippocampal progenitor cells,<sup>34</sup> whereas depletion of HSP27 facilitates apoptosis in bladder cancer UMUC-3 cells induced by paclitaxel.<sup>35</sup> Moreover, a recent study has shown that the expression level of HSP27 in neuroblastoma cells negatively correlates with their sensitivity to FK228.<sup>36</sup> In this study, HSP27 was regulated by FK228 and SAHA in a manner consistent with HDACi sensitivity in cancer cells, but HSP27 is not the target protein mediating FK228-induced cytotoxicity at least in NSCLC cells since either forced overexpression HSP27 or depletion of HSP27 via siRNA had no effect on FK228-induced apoptosis.

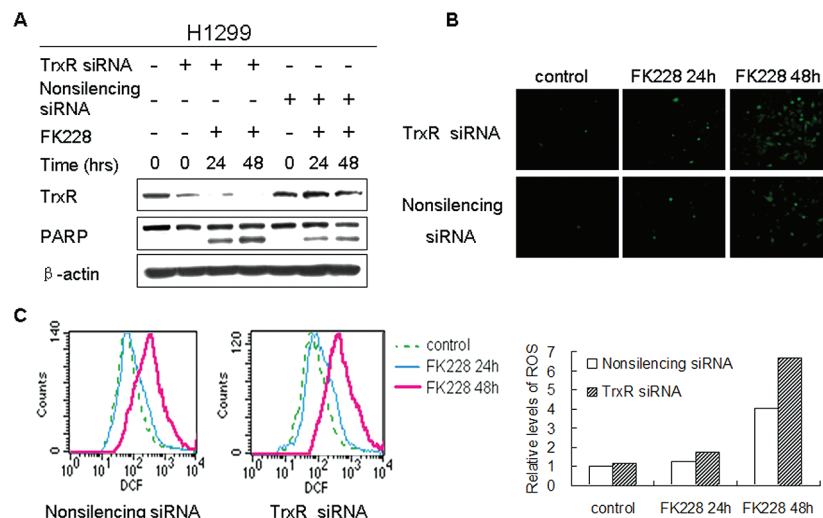


**Figure 7.** Effect of TrxR on FK228-induced ROS accumulation and apoptosis. (A) Effect of TrxR depletion on FK228-induced apoptosis. H1299 cells were transfected with 100 nM TrxR siRNA or nonsilencing siRNA for 48 h and then treated with (+) or without (-) 25 ng/mL FK228 for the indicated times. Protein levels of TrxR and PARP were analyzed by Western blotting;  $\beta$ -actin was used as loading control. The effect of TrxR on FK228-induced ROS accumulation was determined by fluorescence microscopy (B) and flow cytometry (C). H1299 cells were transfected with 100 nM TrxR siRNA or nonsilencing siRNA for 48 h and then treated with (+) or without (-) 25 ng/mL FK228 for the indicated times. Cells were incubated with DCFH-DA for 1 h at 37 °C, washed with PBS three times and analyzed by fluorescence microscopy or flow cytometry.

ROS usually accumulate in the tumor cells treated with chemotherapeutic agents and initiate apoptosis by inducing oxidative injury.<sup>37,38</sup> Several HDACi, including SAHA, MS-275, TSA, NSC3852, LAQ824 and VA, are reported to kill tumor cells by inducing ROS accumulation.<sup>1,37,39–43</sup> As ROS were cleared by the antioxidant enzymes and proteins including superoxide dismutase (SOD), catalase (CAT), thioredoxin (Trx) and glutathione peroxidase (GPx),<sup>44</sup> downregulation of SOD, GPx and Trx play a key role in mediating the lethality induced by oxidative stress in leukemia cells treated with SAHA or sodium butyrate.<sup>37</sup> TrxR is the reductase of Trx and efficiently scavenges ROS by reducing hydrogen peroxide ( $H_2O_2$ ) directly or Trx and other antioxidant proteins indirectly.<sup>19,45</sup> Moreover, TrxR has been identified as a novel molecular target in cancer therapy since it is overexpressed or constitutively active in many kinds of tumor cells, promoting proliferation and enhancing resistance to chemotherapeutic agents.<sup>46</sup> In this study, we found that the expression level of TrxR is negatively correlated with ROS accumulation, DNA damage, and apoptosis, indicating that TrxR is involved in regulating FK228-induced apoptosis. Moreover, FK228-induced a differential regulation of TrxR in sensitive and resistant cancer cells, and the manner of regulation is very similar to another important antioxidant, Trx. SAHA upregulates Trx expression in resistant normal fibroblast cells, but downregulates Trx in sensitive tumor cells.<sup>10</sup> The mechanisms behind this differential regulation are still undefined, but it is clear that these differential changes correlate well with HDACi sensitivity in cancer cells. Thus, proteome analysis can provide new information about the target proteins involved in HDACi-induced cancer cell cytotoxicity.

## Materials and Methods

**Cells and Reagents.** Human NSCLC cell lines H322 and H1299 and prostate cancer cell lines LNCaP and PC-3 were obtained from the American Tissue Culture Collection (Manassas, VA). FK228 was kindly offered by Dr. David S. Schrump (Thoracic Oncology, Surgery Branch, NIH/NCI). Suberoylanilide

hydroxamic acid (SAHA) was provided by AstraZeneca Company (Macclesfield, SK, U.K.). Z-VAD-FMK was purchased from R&D Systems, Inc. (Minneapolis, MN).

**Cell Growth Assay.** Cells were seeded into 96-well plates ( $5 \times 10^4$  cells per well). After 24 h, cells were treated with or without 25 ng/mL FK228 for the indicated times. Cell growth and viability were evaluated by MTT assay. The absorbance of OD 492 was determined and results are presented as mean  $\pm$  SD of three independent experiments.

**Apoptosis Analysis.** Apoptosis was determined by Annexin V-FLUOS kit (Roche, Indianapolis, IN) according to the manufacturer's instruction. Briefly, cells were cultured with or without 25 ng/mL FK228 for the indicated times and collected by trypsinization. After washing with PBS, cells were stained with annexin V-FITC and propidium iodide and apoptosis was determined by flow cytometry.

**Clonogenic Survival Assay.** One thousand H322 or H1299 cells were plated per well in 6-well plates for 72 h and followed by the treatment of FK228 for the indicated times. Cells were washed, fresh culture fluid was added and colonies were stained with crystal violet 12 days later.

**Western Blot Analysis.** Western blotting was performed according to the method described by Yu et al.<sup>9</sup> Briefly, cells were lysed in laemmli buffer (Bio-Rad Laboratories, CA) and protein lysate concentration was quantified by bicinchoninic acid (BCA) protein assay kit (Pierce, IL). Fifty micrograms of total protein was subjected to SDS-PAGE and transferred onto a PVDF membrane. The membrane was blotted with antibodies for 12–15 h at 4 °C and incubated with horseradish peroxidase-conjugated secondary antibody for 1 h at room temperature. Proteins were detected using the Supersignal West Pico Detection system (Pierce, IL). The antibodies used in the study were anti-PARP, cleaved caspase-3, acetyl-histone H3 (lys9) and Trx (Cell Signaling, Beverly, MA); anti-CRT and G3BP (Abcam, Cambridge, MA); anti-TrxR and HMGB1 (Upstate, Lake Placid, NY); anti-GRB2 (BD bioscience, San Jose, CA); anti-HSP27

(Stressgen, Victoria, British Columbia, Canada) and anti- $\beta$ -actin (Oncogene, Boston, MA).

**Semiquantitative RT-PCR.** Total RNA was isolated by TRIzol reagent (Invitrogen, Carlsbad, CA) and reversely transcribed into cDNA by RevertAid First Strand cDNA Synthesis Kit (Fermentas, Glen Burnie, MD) according to the manufacturer's instruction. The specific primers for genes in the study were designed with primer premier 5.0. PCR was performed for different cycles according to the abundance of genes. The following primer pairs were used for RT-PCR: FBP, 5'-agaaacactggctgacaaac-3' and 5'-agtgccttgaccctcac-3'; PKM2, 5'-ggagaacagccaaagg-3' and 5'-gcacagcacaggaaat-3'; CRT, 5'-atcccacagactcca-3' and 5'-tcctcagcgatgcctca-3'; HMGB1, 5'-tcggaggaggataaga-3' and 5'-ggccgatactcagagcaga-3'; HSP27, 5'-tgtccctggatgtcaacc-3' and 5'-ggatggtgatctcgftgact-3'; G3BP, 5'-gacccatcgccgatcaaag-3' and 5'-tcgacattcagacggac-3'; TrxR, 5'-ctccttggatatggctg-3' and 5'-gcgtgttgcacagacaatgt-3'; RCN1, 5'-gatgtccacgtgatgag-3' and 5'-gaggatccatgttgc-aaatctc-3'; hnRNP K, 5'-cccgatagggttagtgc-3' and 5'-attgca-gagtcccaagttc-3'; GRB2, 5'-gcttcattccaagaactac-3' and 5'-gaacctcaccaccaggag-3'; G3PDH, 5'-accacagtccatgc-ccatcac-3' and 5'-tccaccaccctgtgt-3'.

**Proteomic Assay.** FK228-induced differentially expressed proteins were identified by 2-DE and MALDI-TOF-MS according to the method described by Jin et al.<sup>47</sup> Briefly, cells were lysed by sonication in lysis buffer (8 M UREA, 4% CHAPS, 40 mM Tris, 1 mM EDTA, 1 mM EGTA, 60 mM DTT) and protein lysate concentration was determined by Bradford Method. 2D-PAGE was performed by a two-dimensional electrophoresis system (Amersham Pharmacia Biotech, Uppsala, Sweden). Protein samples were subjected to IEF by IPG-strips (pH 3–10 nonlinear, 18 cm, GE Healthcare) with a total 80 000 V·h. After equilibration, IPG-strips were subjected to second-dimension separation on 13% SDS-polyacrylamide gels. Protein spots were detected by silver (130  $\mu$ g of protein load) and Coomassie Blue R-250 (1500  $\mu$ g of protein load) staining and analyzed by the software of ImageMaster 2D platform. The differentially expressed protein spots were excised from coomassie blue stained 2-D gels and digested by modified sequence grade trypsin. The extracted peptides were analyzed by MALDI-TOF-MS (Bruker-Franzen, Bremen, Germany) to obtain the data of PMF. The differentially expressed proteins were identified with significant values ( $p < 0.05$ ) by searching the PMF through the Swiss-Prot and NCBInr databases with Mascot search engine. According to biological function, the identified proteins were classified into five clusters.

**Measurement of TrxR Activity.** The activity of TrxR was measured by Thioredoxin Reductase Assay Kit (Cayman chemical, Ann Arbor, MI) according to the manufacturer's instruction. Briefly, cells were collected by scraping and homogenized in cold buffer (50 mM potassium phosphate and 1 mM EDTA, pH 7.4) on ice. The protein concentration in the supernatant of lysate was determined by BCA protein assay kit (Pierce, IL). Protein samples (3 mg/mL), NADPH and DTNB were added to assay buffer in 96-well plates and gently mixed. The absorbance of the mixture was read once every minute at 405 nm to obtain the data at eight time point which was used to calculate the activity of TrxR according to the equation described in the manual. The TrxR activity was analyzed by SPSS and test with One-Way ANOVA. The value of significance is 0.05.

**ROS Measurements.** ROS were evaluated by reactive oxygen species assay kit (Applygen Technologies, Inc., Beijing, China)

according to the manufacturer's instruction. Briefly, cells were incubated with 3  $\mu$ M DCFH-DA for 1 h at 37 °C and ROS measurements were determined by fluorescence microscope or flow cytometry at an excitation wavelength of 480 nm and an emission wavelength of 525 nm. The relative fluorescence ratio was calculated based on the mean geometry fluorescence determined by flow cytometry and shown as histogram.

**Measurement of Phospho-H2AX (ser139).** Cells were collected by trypsinization and fixed with 2% formaldehyde for 10 min at 37 °C. The fixed cells were permeabilized with 90% methanol on ice for 30 min, blocked with 0.5% BSA for 10 min at room temperature and incubated with Phospho-Histone H2AX (Ser139) (Alexa Fluor 647 Conjugate) (Cell Signaling, Beverly, MA) antibody in the dark for 1 h at room temperature. The labeled cells were determined by flow cytometry.

**Cell Transfection.** The plasmid of wild-type human HSP27 (GenBank accession no.: X54079) and empty plasmid (pRetro Tet-On) were constructed and kindly offered by Kyungjin Kim.<sup>34</sup> H322 cells were seeded at  $6 \times 10^5$  cells per well in 6-well plates. After 24 h, cells were transfected with wild-type human HSP27 plasmid or empty plasmid with VigoFect (Vigorous Biotechnology, Inc., Beijing, China) according to the manufacturer's instruction. The 21-nt duplex siRNA for HSP27 (target sequence of 5'-aagctgcaaatccgatgaga-3') and nonsilencing siRNA (target sequence of 5'-ttcccgaaatgttgcacgt-3') were synthesized by Shanghai GeneChem, Inc. (Shanghai, China), but siRNA for TrxR was obtained from Santa Cruz Biotechnology (Santa Cruz, CA.). H1299 cells were plated at  $4 \times 10^5$  cells per well in 6-well plates. After 24 h, cells were transfected with 100 nM HSP27 siRNA, TrxR siRNA or nonsilencing siRNA using RNAiFect (QIAGEN GmbH, Hilden, Germany) according to the manufacturer's instruction.

**Abbreviations:** HDACi, Histone deacetylase inhibitors; SAHA, suberoylanilide hydroxamic acid; ROS, reactive oxygen species; Trx, thioredoxin; TrxR, thioredoxin reductase; PARP, poly (ADP-ribose) polymerase; siRNA, small interfering RNA; CRT, calreticulin.

**Acknowledgment.** We thank Kyungjin Kim for providing the vectors of wild-type HSP27. This work was supported by Grants 30330620 and 30470898 from the National Natural Science Foundation of China (to X.Y.).

## References

- Martirosyan, A.; Leonard, S.; Shi, X.; Griffith, B.; Gannett, P.; Strobl, J. *J. Pharmacol. Exp. Ther.* **2006**, *317*, 546–552.
- Butler, L. M.; Zhou, X.; Xu, W. S.; Scher, H. I.; Rifkind, R. A.; Marks, P. A.; Richon, V. M. *Proc. Natl. Acad. Sci. U.S.A.* **2002**, *99*, 11700–11705.
- Shao, Y.; Gao, Z.; Marks, P. A.; Jiang, X. *Proc. Natl. Acad. Sci. U.S.A.* **2004**, *101*, 18030–18035.
- Glaser, K. B. *Biochem. Pharmacol.* **2007**, *74*, 659–671.
- Acharya, M. R.; Sparreboom, A.; Venitz, J.; Figg, W. D. *Mol. Pharmacol.* **2005**, *68*, 917–932.
- Peart, M. J.; Smyth, G. K.; van Laar, R. K.; Bowtell, D. D.; Richon, V. M.; Marks, P. A.; Holloway, A. J.; Johnstone, R. W. *Proc. Natl. Acad. Sci. U.S.A.* **2005**, *102*, 3697–3702.
- Sasakawa, Y.; Naoe, Y.; Sogo, N.; Inoue, T.; Sasakawa, T.; Matsuo, M.; Manda, T.; Mutoh, S. *Biochem. Pharmacol.* **2005**, *69*, 603–616.
- Glozak, M. A.; Sengupta, N.; Zhang, X.; Seto, E. *Gene* **2005**, *363*, 15–23.
- Yu, X.; Guo, Z. S.; Marcu, M. G.; Neckers, L.; Nguyen, D. M.; Chen, G. A.; Schrump, D. S. *J. Natl. Cancer Inst.* **2002**, *94*, 504–513.
- Ungerstedt, J. S.; Sowa, Y.; Xu, W. S.; Shao, Y.; Dokmanovic, M.; Perez, G.; Ngo, L.; Holmgren, A.; Jiang, X.; Marks, P. A. *Proc. Natl. Acad. Sci. U.S.A.* **2005**, *102*, 673–678.
- Shigematsu, N.; Ueda, H.; Takase, S.; Tanaka, H.; Yamamoto, K.; Tada, T. *J. Antibiot.* **1994**, *47*, 311–314.

- (12) Xu, W.; Ngo, L.; Perez, G.; Dokmanovic, M.; Marks, P. A. *Proc. Natl. Acad. Sci. U.S.A.* **2006**, *103*, 15540–15545.
- (13) Zhao, Y.; Tan, J.; Zhuang, L.; Jiang, X.; Liu, E. T.; Yu, Q. *Proc. Natl. Acad. Sci. U.S.A.* **2005**, *102*, 16090–16095.
- (14) Insinga, A.; Monestiroli, S.; Ronzoni, S.; Gelmetti, V.; Marchesi, F.; Viale, A.; Altucci, L.; Nervi, C.; Minucci, S.; Pelicci, P. G. *Nat. Med.* **2005**, *11*, 71–76.
- (15) Sandor, V.; Bakke, S.; Robey, R. W.; Kang, M. H.; Blagosklonny, M. V.; Bender, J.; Brooks, R.; Piekarz, R. L.; Tucker, E.; Figg, W. D.; Chan, K. K.; Goldspiel, B.; Fojo, A. T.; Balcerzak, S. P.; Bates, S. E. *Clin. Cancer Res.* **2002**, *8*, 718–728.
- (16) Parker, C.; Molife, R.; Karavasilis, V.; Reid, A.; Patterson, S. G.; Riggs, C.; Higano, C.; Stadler, W. M.; McCulloch, W.; de Bono, J. S. *J. Clin. Oncol.* **2007**, *25*, 15507.
- (17) Mazurek, S.; Grimm, H.; Boschek, C. B.; Vaupel, P.; Eigenbrodt, E. *Br. J. Nutr.* **2002**, *87*, 23–29.
- (18) Bruey, J. M.; Ducasse, C.; Bonniaud, P.; Ravagnan, L.; Susin, S. A.; Diaz-Latoud, C.; Gurbuxani, S.; Arrigo, A. P.; Kroemer, G.; Solary, E.; Garrido, C. *Nat. Cell Biol.* **2000**, *2*, 645–652.
- (19) Nordberg, J.; Arner, E. S. *Free Radical Biol. Med.* **2001**, *31*, 1287–1312.
- (20) Ding, W.; Hudson, L. G.; Liu, K. *J. Mol. Cell. Biochem.* **2005**, *279*, 105–112.
- (21) Burma, S.; Chen, B. P.; Murphy, M.; Kurimasa, A.; Chen, D. *J. Biol. Chem.* **2001**, *276*, 42462–42467.
- (22) Waterman, H.; Katz, M.; Rubin, C.; Shtiegman, K.; Lavi, S.; Elson, A.; Jovin, T.; Yarden, Y. *EMBO J.* **2002**, *21*, 303–313.
- (23) Choi, J. H.; Hong, W. P.; Yun, S.; Kim, H. S.; Lee, J. R.; Park, J. B.; Bae, Y. S.; Ryu, S. H.; Suh, P. G. *Cell Signalling* **2005**, *17*, 1289–1299.
- (24) Groenendyk, J.; Lynch, J.; Michalak, M. *Mol. Cells* **2004**, *17*, 383–389.
- (25) Okunaga, T.; Urata, Y.; Goto, S.; Matsuo, T.; Mizota, S.; Tsutsumi, K.; Nagata, I.; Kondo, T.; Ihara, Y. *Cancer Res.* **2006**, *66*, 8662–8671.
- (26) Pike, S. E.; Yao, L.; Setsuda, J.; Jones, K. D.; Cherney, B.; Appella, E.; Sakaguchi, K.; Nakhasi, H.; Atreya, C. D.; Teruya-Feldstein, J.; Wirth, P.; Gupta, G.; Tosato, G. *Blood* **1999**, *94*, 2461–2468.
- (27) Sheard, M. A.; Vojtesek, B.; Simickova, M.; Valik, D. *J. Cell. Biochem.* **2002**, *85*, 670–677.
- (28) Dohmoto, K.; Hojo, S.; Fujita, J.; Yang, Y.; Ueda, Y.; Bandoh, S.; Yamaji, Y.; Ohtsuki, Y.; Dobashi, N.; Ishida, T.; Takahara, J. *Int. J. Cancer* **2001**, *91*, 468–473.
- (29) Notari, M.; Neviani, P.; Santhanam, R.; Blaser, B. W.; Chang, J. S.; Galietta, A.; Willis, A. E.; Roy, D. C.; Caligiuri, M. A.; Marcucci, G.; Perrotti, D. *Blood* **2006**, *107*, 2507–2516.
- (30) Lynch, M.; Chen, L.; Ravitz, M. J.; Mehtani, S.; Korenblat, K.; Pazin, M. J.; Schmidt, E. V. *Mol. Cell. Biol.* **2005**, *25*, 6436–6453.
- (31) Irvine, K.; Stirling, R.; Hume, D.; Kennedy, D. *Int. J. Dev. Biol.* **2004**, *48*, 1065–1077.
- (32) Liu, J.; Kouzine, F.; Nie, Z.; Chung, H. J.; Elisha-Feil, Z.; Weber, A.; Zhao, K.; Levens, D. *EMBO J.* **2006**, *25*, 2119–2130.
- (33) Barnes, C. J.; Li, F.; Mandal, M.; Yang, Z.; Sahin, A. A.; Kumar, R. *Cancer Res.* **2002**, *62*, 1251–1255.
- (34) Son, G. H.; Geum, D.; Chung, S.; Park, E.; Lee, K. H.; Choi, S.; Kim, K. *Biochem. Biophys. Res. Commun.* **2005**, *338*, 1751–1758.
- (35) Kamada, M.; So, A.; Muramaki, M.; Rocchi, P.; Beraldi, E.; Gleave, M. *Mol. Cancer Ther.* **2007**, *6*, 299–308.
- (36) Keshelava, N.; Davicioni, E.; Wan, Z.; Ji, L.; Spoto, R.; Triche, T. J.; Reynolds, C. P. *J. Natl. Cancer Inst.* **2007**, *99*, 1107–1119.
- (37) Gao, N.; Rahmani, M.; Shi, X.; Dent, P.; Grant, S. *Blood* **2006**, *107*, 241–249.
- (38) Miller, C. P.; Ban, K.; Dujka, M. E.; McConkey, D. J.; Munsell, M.; Palladino, M.; Chandra, J. *Blood* **2007**, *110*, 267–277.
- (39) Rosato, R. R.; Maggio, S. C.; Almenara, J. A.; Payne, S. G.; Atadja, P.; Spiegel, S.; Dent, P.; Grant, S. *Mol. Pharmacol.* **2006**, *69*, 216–225.
- (40) Kawai, Y.; Arinze, I. *J. Cancer Res.* **2006**, *66*, 6563–6569.
- (41) Rueffli, A. A.; Ausserlechner, M. J.; Bernhard, D.; Sutton, V. R.; Tainton, K. M.; Kofler, R.; Smyth, M. J.; Johnstone, R. W. *Proc. Natl. Acad. Sci. U.S.A.* **2001**, *98*, 10833–10838.
- (42) Rosato, R. R.; Almenara, J. A.; Grant, S. *Cancer Res.* **2003**, *63*, 3637–3645.
- (43) Donadelli, M.; Costanzo, C.; Beghelli, S.; Scupoli, M. T.; Dandrea, M.; Bonora, A.; Piacentini, P.; Budillon, A.; Caraglia, M.; Scarpa, A.; Palmieri, M. *Biochim. Biophys. Acta* **2007**, *1773*, 1095–1106.
- (44) Andreyev, A. Y.; Kushnareva, Y. E.; Starkov, A. A. *Biochemistry (Moscow)* **2005**, *70*, 200–214.
- (45) Arner, E. S.; Holmgren, A. *Eur. J. Biochem.* **2000**, *267*, 6102–6109.
- (46) Nguyen, P.; Awwad, R. T.; Smart, D. D.; Spitz, D. R.; Gius, D. *Cancer Lett.* **2006**, *236*, 164–174.
- (47) Jin, B. F.; He, K.; Wang, H. X.; Bai, B.; Zhou, T.; Li, H. Y.; Man, J. H.; Liu, B. Y.; Gong, W. L.; Wang, J.; Li, A. L.; Zhang, X. M. *J. Proteome Res.* **2006**, *5*, 2815–2823.

PR7008753